

System Noise Technology Roadmaps for a Transonic Truss-Braced Wing and Peer Conventional Configuration

Jason C. June*, Russell H. Thomas†, Yueping Guo‡
NASA Langley Research Center, Hampton, VA 23681, USA

A system noise assessment is performed for a Boeing-designed Transonic Truss-Braced Wing, resized using NASA tools in order to estimate the performance of the configuration relative to NASA noise goals. For comparison, a conventional configuration with comparable mission requirements, technology assumptions, and design assumptions is also assessed. Following the baseline noise assessments, a noise reduction technology roadmap is developed from technologies expected to mature to an appropriate technology readiness level by the targeted entry into service date. Noise prediction of both baseline configurations shows a 4.7 EPNdB cumulative certification advantage for the Transonic Truss-Braced Wing. Both configurations fall short of the mid term NASA noise goal, even with application of the noise reduction technologies in the roadmap. The roadmap provides 7.3 EPNdB of cumulative noise reduction for the conventional configuration and 7.8 EPNdB for the Transonic Truss-Braced Wing.

Nomenclature

c = chord
 C = coefficient
 D = drag
 H = average aft-duct annular height
 L = lift
 \mathbb{L} = acoustically lined length
 R = inlet radius

Subscripts

l = lift
 max = maximum
 $rotor$ = rotor
 t = tip

I. Introduction

THE NASA Aeronautics Research Mission Directorate has continually supported research focused on technologies that drive efficiency gains and reductions in aircraft emissions. Details of aggressive noise, fuel/energy consumption, and NO_x goals for ultra-efficient subsonic transports are detailed in its Strategic Implementation Plan [1]. To meet the noise goal for the mid term timeframe (2025–2035), noise reduction technologies resulting in 25–35 EPNdB cumulative margin** must be matured to a technology readiness level (TRL) of 5–6. One such technology of interest in working toward the fuel consumption goal is a configuration change from a cantilevered wing to a truss-braced wing to enable improved efficiency through an increase in the wing aspect ratio. While the potential for reduced fuel consumption is clear, the related impacts on noise reduction require additional analysis. This work addresses noise considerations for a Transonic Truss-Braced Wing (TTBW) configuration and assesses whether there is a path to meeting the NASA noise goal.

*Research Aerospace Engineer, Aeroacoustics Branch, MS 461, AIAA Member

†Senior Research Engineer, Aeroacoustics Branch, MS 461, AIAA Associate Fellow

**Unless otherwise noted, all cumulative margins are relative to minimum required margin to meet FAA Stage 5 regulations (equivalent to ICAO Chapter 14).

Research into enabling high aspect ratio wings has occurred under ONERA's Aile Laminaire haUBAnée à Traînée Réduite par Optimisation multidisciplinaire (ALBATROS) project [2]. The ALBATROS configuration has a single-aisle mission characterized by a payload of 180 passengers, a design mission of 3000 NM, economic mission of 500 NM, and cruise speed of Mach 0.75 at 39,000 ft. The design has a strut-braced (no jury strut) high wing with a pair of engines mounted to the rear of the fuselage. The strut-braced configuration was estimated to have a 7% reduction in fuel weight over a cantilever wing design. However, to the knowledge of the authors, no system noise assessment of this concept was performed.

More recently, as part of Clean Sky 2, the Ultra High Aspect Ratio Wing Advanced Research and Designs (U-HARWARD) project is studying three different implementation paths [3]: increased aspect ratios for conventional, cantilevered wing designs, an additional research spiral into the ALBATROS strut-braced wing configuration, and a folding wingtip technology that has developed into Airbus' AlbatrosONE demonstrator. While some aeroacoustic research is planned, no system noise assessment efforts have been mentioned.

Significant development of a Boeing-designed concept has occurred through an ongoing, multiphase, NASA-funded contract, Subsonic Ultra-Green Aircraft Research (SUGAR). In the first phase [4], three unconventional concepts were proposed for an entry into service (EIS) date of 2030–2035, along with two conventional configurations: one with the same future EIS, and one to serve as a current-day (2008) baseline. Two of the three unconventional configurations were truss-braced wing designs: the SUGAR High and the SUGAR Volt, an electric propulsion variant of the SUGAR High.

A technology roadmap was developed, and risk assessments of the technologies needed for each concept to reach the NASA goals were performed. Three broad categories of technologies were proposed for the noise goal: passive engine treatments, active noise control and fluidics, and airframe acoustic technologies. The passive engine treatments were expected to provide the most benefit. However, the need for additional noise reduction technologies was noted since none of the concepts met the NASA goal at that time, which was limiting the day-night average sound level 55 dBA noise contour within a typical airport boundary.

This conclusion was supported by a fleet noise analysis using the FAA's Integrated Noise Model and noise-power-distance (NPD) data. In order to meet the noise contour goal for the projected 2055 fleet size, it was found that a fleet comprising only N+3 concepts required a –45 EPNdB cumulative certification noise reduction relative to the baseline (2008 fleet) aircraft. However, an assessment of the technologies assumed to be on the SUGAR High only corresponded to a –22 EPNdB cumulative reduction relative to the baseline configuration.

In Phase II [5], additional noise assessments of the certification noise were performed on the SUGAR High and SUGAR Volt. Parametric, component-level tools were used to calculate the airframe noise. A General Electric GENx-1B NPD database was modified for use in calculating the engine noise, and incoherently summed with the airframe noise at the certification observer locations to determine the total system noise. The SUGAR High configuration was estimated to have a 15.8 EPNdB (reported as 22.8 EPNdB to Stage 4) cumulative margin. Additionally, a parametric study was done as an initial step toward a detailed acoustic technology roadmap. After considering a list of candidate technologies, the total noise reduction potential was estimated for both the engine and airframe subsystems, resulting in a maximum of 2 EPNdB and 3 EPNdB, respectively. When these reductions were propagated to the system level, the cumulative margin was increased to 23.1 EPNdB (30.1 EPNdB to Stage 4). On approach, the main contributors to the system noise were the landing gear and flap noise. For the takeoff certification points, the fan, jet, and flap were the primary sources.

Phase III [6] and Phase IV [7] work has been focused on iterating the aerodynamic design to higher cruise Mach numbers, from 0.7 in Phase II to 0.8 in Phase IV. Consequently, there have not been any published system noise assessments during these phases. However, one of the research topics noted by Harrison et al. [7] for risk reduction is to perform an acoustic assessment and develop a roadmap for demonstrating key acoustic technologies.

This paper presents a system noise assessment of the certification noise levels for a NASA derivative of the Phase IV SUGAR Transonic Truss-Braced Wing configuration. Additionally, a technology roadmap is applied to the TTBW in an effort to gauge the noise reduction potential of this configuration with technologies that can be sufficiently matured in the mid term timeframe. The assessment and roadmap are also applied to a conventional configuration that serves as a point of comparison under the same design constraints and methodology. Following a more detailed description of the two configurations, the process used for the baseline noise prediction and noise reduction roadmap are laid out. The salient results of each portion of the study are then presented, ending with conclusions and suggestions for future work.

II. Configuration Descriptions

As mentioned previously, two configurations are used in this paper: a resized derivative of the Boeing-designed Phase IV TTBW, and a conventional configuration (CC) with the same technology assumptions and EIS date. Matching

these parameters enable the extraction of relative performance due solely from the reconfiguration to a TTBW, as noted in the recommendations of Bradley and Droney [5]. Both vehicles have the same design mission: transporting 154 passengers 3500 NM at a cruise Mach of 0.8. The derivative TTBW is resized from the Boeing design point using NASA mission analysis tools, the FLight OPTimization System (FLOPS) [8] and Numerical Propulsion Simulation System (NPSS) [9] to meet a minimum fuel burn requirement. A similarly resized, higher aspect ratio version of the N3CC [10] is used as the conventional configuration. Table 1 summarizes some relevant design parameters for both concepts.

The propulsion system for both configurations is the gFan+ [5, 6], a direct drive, gas turbine with eighteen fan blades and forty stator blades, and a rotor-stator spacing of $1.9c_{rotor}$. It has a fan pressure ratio of 1.4 on full-power takeoff. Acoustic lining is applied to the inlet, interstage, and aft sections of length $0.7R$, $0.3H$, and $3.2H$, respectively.

The gFan+ engine cycle is an optimized fit to the publicly available information provided in the SUGAR reports (not an identical model), with modifications to account for the updated cruise requirements. The calibration procedure and tools for the propulsion model are detailed in Thacker and Blaesser [11].

Table 1 Design parameters are summarized for both vehicle concepts.

| Dimension | TTBW | CC | Units |
|------------------------------------|---------|---------|-------|
| Span | 158.1 | 123.7 | ft |
| Aspect Ratio | 19.6 | 13.1 | – |
| Gross Takeoff Weight | 135,600 | 136,200 | lb |
| Maximum Landing Weight | 116,600 | 114,400 | lb |
| Sea Level Static Thrust per Engine | 23,200 | 21,800 | lb |
| Fan Diameter | 72.5 | 70.4 | in |

Apart from the engine definition, a considerable amount of geometric information on the layout of airframe components is also required to perform a noise assessment. Dickey and Beyar [12] detail the development of a high-lift system that is compatible with a laminar flow wing and mission requirements. Figure 1 shows the general layout: a leading edge variable camber Krueger, and a single-segment flap with outboard ailerons. The detail in this layout is atypical in a noise assessment of a conceptual aircraft, as many of the parameters are well-defined; both two- and three-dimensional design cycles have been completed for the leading- and trailing-edge devices. The two-dimensional design considered several types of leading edge devices, along with the rigging (e.g., gap, deployment angle) of the preferred leading edge and trailing edge devices to maximize L/D on takeoff and $C_{L,max}$ on landing as design objectives. In general, these objectives are well-aligned with noise objectives. A high takeoff L/D leads to an improved climb rate, and therefore, larger propagation distances to ground observers, while a higher $C_{L,max}$ reduces the approach velocity. The three-dimensional analysis identified the need to rig the Krueger at different angles on the outboard section. Geometric similarity of the resulting Boeing high-lift design is assumed for the TTBW design here, and dimensions are scaled by the wingspan and chord ratios between the Boeing and NASA design points as appropriate.

A more common situation for a conceptual aircraft is the incomplete geometric definition of the high-lift system planform or rigging (gaps, deflection angle, etc.). For these cases, a donor aircraft high-lift system must be identified in order to scale the geometry to the concept under study. These donor high-lift systems may represent in-service aircraft, or concepts from databases where sufficient geometric definition exists. Although the planform of the conventional configuration was defined by Boeing, the reports did not include the rigging parameters, so a similar design on an unpublished, single-aisle concept from a Boeing database developed in previous work was utilized.

The landing gear definition for noise prediction is handled similarly to the high-lift surfaces. For both configurations, the requisite information is available for all dimensions with the exception of the diameters of the gear struts. These values are linearly interpolated as a function of maximum takeoff weight from the database mentioned in the previous paragraph.

III. Noise Prediction Process

For this work, the internal research version of the Aircraft NOise Prediction Program (ANOPP) L31v9 is utilized, running within the ANOPP2 framework [15]. The research version contains several additional noise source prediction methods that are not available in the publicly released version of ANOPP. In particular, a suite of airframe element

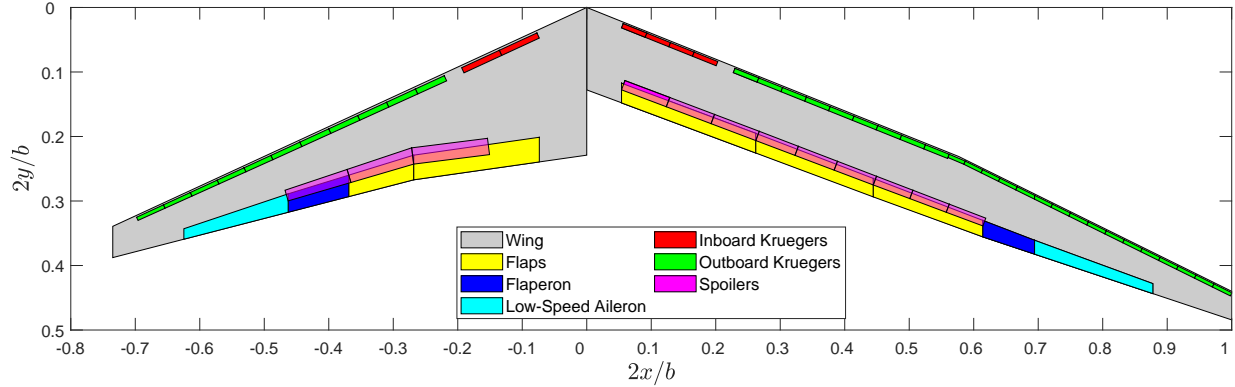


Fig. 1 High-lift system layout for the conventional configuration (left) and TTBW (right) [13, 14]. Coordinates are normalized by the semispan of the TTBW.

prediction methods are available, enabling prediction of Krueger leading edge devices.

As mentioned in Section II, an engine deck is developed in NPSS, and the airframe sizing and flight path are generated from FLOPS, yielding the aircraft geometry, relative source positions, and engine states required for noise predictions. Using this information, source noise predictions of nearly all elements are handled within ANOPP using parametric models. However, the propulsion airframe aeroacoustic (PAA) effects and the effects of some technologies are predicted using computational or experimental databases. More information on the methods used to incorporate any particular technology can be found in previous noise roadmap studies [16–19] and are excluded here for brevity.

For the individual acoustic sources, the three main engine source elements are considered: the fan, core, and jet. The engine noise is predicted using Krejsa and Stone [20] to update the correlations from the original Heidmann [21] fan model for more modern designs with lower fan pressure ratios. The effects of the acoustic liner are predicted using an in-house LINER module, which is a modified version of the GE TREAT model [22]. One modification of note is the extension to model multidegree-of-freedom (MDOF) liners, rather than the assumed installation of double-degree-of-freedom inlet and single-degree-of-freedom aft liner present in the original TREAT model. The core noise is computed using the GECOR module [23], and the updated version [24] of the Stone model, ST2JET, is used to estimate the jet noise.

The airframe noise comprises the prediction of four source elements: the landing gear, trailing edge, flap side edge, and leading edge Krueger. Updated versions of the Guo models with several minor modifications are used for landing gear [25] and leading edge noise [26] in the present work. The prediction of the interaction effects between the landing gear and the local flow was also decoupled from the landing gear source noise prediction, so that each can be predicted as needed. This is particularly important for the TTBW landing gear, which is subject to a flow field that is markedly different from the conventional configuration. An unpublished model by Guo following a similar framework was used to predict the flap side-edge noise. Last, the trailing edge noise is predicted using the Fink model [27]. The trailing edge noise is calculated for the wing, empennage, and strut.

Certification procedures, outlined in 14 Code of Federal Regulations (CFR), Part 36 [28], are used herein to consistently assess the performance of each aircraft. Certification consists of measuring the noise at three observer locations that collectively represent near-airport operating conditions: approach, full power departure (lateral), and departure engine cutback (flyover). The observer locations are shown in Figure 2, along with details of the process for determining the effective perceived noise level (EPNL), a noise metric that incorporates some characteristics of human annoyance. Duration is accounted for by integration of the time history of the tone corrected perceived noise level (PNLT), which in turn accounts for noise amplitude, spectral character, and the nonlinear sensitivity of the human ear. In order to meet the current certification requirements, the measured levels must be less than the maximum allowable limit for each point. These limits are defined in Stage 3 as a function of maximum certificated takeoff mass/weight and the number of engines. An additional constraint is levied on the cumulative level (i.e., the algebraic sum of the three certification levels). For Stage 5, the cumulative margin, calculated as the difference of the cumulative level from the sum of the individual maximum allowable limits, must be a minimum of 17 EPNdB. As noted in Section I, the NASA goals are relative to this minimum required Stage 5 margin, rather than the margin to the maximum limits.

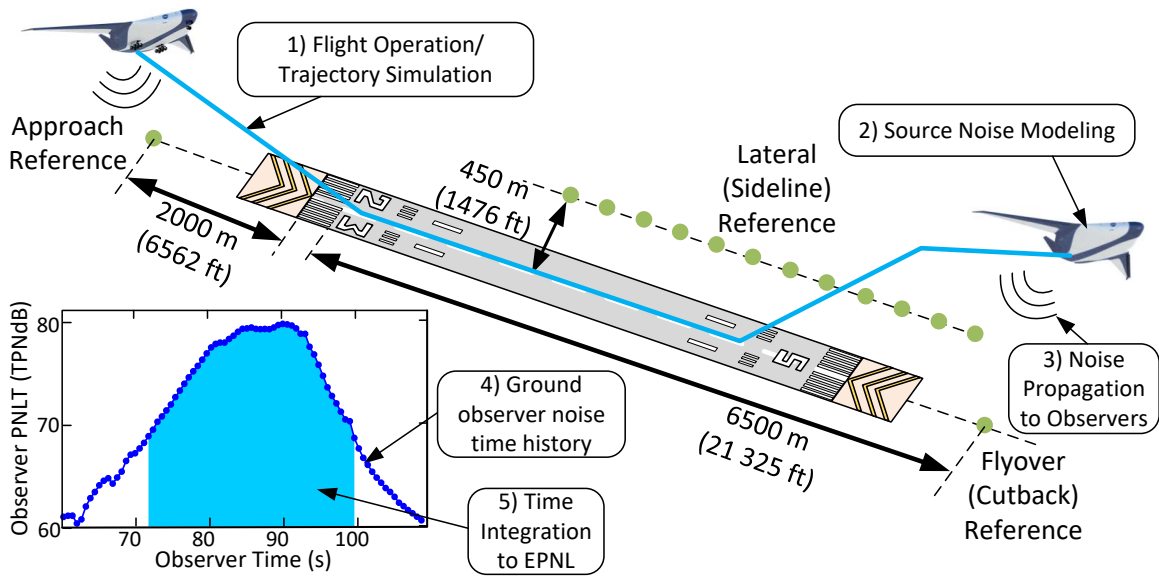


Fig. 2 The location of the certification points along with an overview of the process of obtaining an EPNL from a prediction.

IV. Noise Technology Roadmap

The baseline prediction described in Section III matches the noise technology assumptions applied in the SUGAR work as closely as possible. The Phase II noise assessment described in Section I noted that a list of noise technologies were proposed by Boeing and added to the baseline vehicle to assess the noise benefit. The roadmap here follows an independent, but similar process. Literature was surveyed for noise reduction technologies that could be developed to a TRL of 5–6 in the mid term timeframe. Additional technologies that could reach the appropriate TRL if they receive increased focus and funding were grouped together as potential mid term technologies. Several NASA-developed technologies were also included based on past work and the clear need and opportunity for additional noise reduction. Many technologies are being matured to address engine noise reduction. A more thorough literature review and details on modeling for several of them can be found in previously published studies [16–19]. Specifically, these are the thickened bifurcation (to allow for placement of acoustic liners), over-the-rotor liner, MDOF liner, acoustically soft outlet guide vanes, and a negatively scarfed inlet for the fan noise. Details can also be found for the center plug liner technology applied to the core noise. Similarly, more favorable PAA effects can be obtained using a liner on the underside of the wing.

Two additional engine technologies have been added for consideration in the intervening years since the past roadmap assessments. PAA chevrons are considered to reduce the jet noise. These are modeled by utilizing scaled data gathered during wind tunnel testing detailed in Thomas et al. [29]. Additionally, an aft cowl liner [30] was considered as an additional technology to reduce aft fan noise, which can be a dominant source, even after application of targeted noise reduction technologies. As an initial model, the aft cowl liner is treated as additional liner area in the aft duct with a 50% reduction applied, to account for the significant differences in the propagation of acoustic energy outside the duct relative to the bypass duct interior, where the technology is effectively applied in this model. Development of a more physical model for this technology is left as future work.

Similarly, past publications [16–19] have discussed several airframe technologies at length. These are the partial main and nose gear fairings, as well as pod landing gear for the landing gear noise, porous flap side edge and continuous moldline treatment for the flap noise, and sealed gaps and a dual-use fairing (fairs both the cove and structural brackets) for the Krueger noise. Lastly, a landing gear door liner is added due to its inclusion in ongoing CLEEN III work [31]. For now, this is modeled here as a 0.25 dB reduction of the main gear noise at all frequencies and directivity angles. Use of more physical tools (e.g., ray tracing) to develop a more realistic estimate are also left as future work.

Similar to prior studies [18, 19], the technologies included in the roadmaps are applied in the order of most to least noise reduction. The first iteration starts by predicting the noise reduction of each individual technology in turn, retaining only the technology that provides the most noise reduction. Following iterations retain the technologies from previous ones that provided maximum noise reduction, while predicting all remaining unapplied technologies to determine the next technology to be retained until the list of technologies is exhausted. This is done with the assumption that, *ceteris paribus*, the technologies with the most noise reduction will most likely be applied first in practical applications on aircraft products, understanding that it is not likely that all possible technologies will be matured by the estimated timeframe due to implementation challenges (i.e., the “-ilities”) [32]. In addition to the “one-on” approach described above, a “one-off” estimate of each technology’s noise reduction is also given by applying all the technologies and computing the difference in cumulative noise with only that particular technology removed. However, for the circumstance where a technology replaces another applied at a previous roadmap iteration, the noise reduction is calculated as the difference between all technologies applied and the noise level without both the technology being considered and the incompatible technology. For example, when calculating the impact of continuous moldline link flap treatment, the quietest configuration is compared to the configuration without both continuous moldline link and porous flap side edge treatment. The other example of technology replacement is the pod gear on the TTBW, which is incompatible with the partial main gear fairing and landing gear door liner. Note that if the relative source ranking does not change considerably throughout the roadmap process, the one-off and one-on estimates are generally comparable.

V. Results

The results of the noise analysis for both the baseline and roadmap configurations of the vehicles are presented below. The baseline vehicle discussion is centered on the inherent qualities of the vehicles, and the advantages of each. Note that the discussion in Section V.A is meant to explain the major differences between the two configurations, but a more formal sensitivity study is needed to determine the exact quantitative impact of each input parameter. Some commentary on the key results of this analysis in context to the previous noise analysis performed in the SUGAR Phase II study are provided next. Last, the roadmap analysis conversation focuses on the impact of individual technologies.

A. Baseline Vehicle Results

The TTBW and CC noise certification levels are predicted for the baseline vehicle configuration described in Section II. These levels, reported in Table 2, show that the TTBW has a cumulative advantage of 4.7 EPNdB over the CC. Also illustrated in the table is the difference in the certification levels when the PAA effects are not predicted for the fan, jet, and core elements. The cumulative PAA benefit is tabulated as the sum of the predicted levels that include PAA effects subtracted from those that do not. A positive PAA benefit indicates the dominance of advantageous PAA effects, e.g., shielding. Negative PAA benefits (penalties) as are present on the CC and the TTBW are due to increased noise at the observers primarily due to reflection from the fuselage and wing. The TTBW is able to reduce the PAA penalty relative to the CC primarily through improved shielding of engine noise at sideline (for 1 EPNdB). The high-wing configuration shifts the engine location toward a position that uses the fuselage more efficiently as a shielding body at high azimuthal angles. At the two certification points under the flight path, the CC fares slightly better than the TTBW with respect to the PAA penalty. Additional investigation and modeling are warranted to understand these results, as it was expected that the shorter chord of the TTBW, in conjunction with the modeled shielding of the wing reflection by the strut over a narrow range of polar angles would generate an additional benefit. It is expected that improved understanding of the relevant physics will provide further opportunities to design for additional reductions in the PAA penalty that may not be available options for a conventional engine-under-wing configuration.

Table 2 The certification levels and cumulative margin, relative to the limits, as well as the minimum Stage 5 margin, are given in units of EPNdB. Additionally, the levels without PAA effects are shown for each individual point, along with the cumulative impact of PAA effects in units of Δ EPNdB.

| Concept | Level with PAA | | | Cumulative Margin (re Limits) | Level without PAA | | | Cumulative PAA Benefit |
|---------|----------------|---------|---------|-------------------------------|-------------------|---------|---------|------------------------|
| | Approach | Flyover | Lateral | | Approach | Flyover | Lateral | |
| TTBW | 84.0 | 75.3 | 92.1 | 18.0 (35.0) | 83.0 | 73.3 | 91.1 | -4.0 |
| CC | 83.8 | 79.9 | 92.5 | 13.3 (30.3) | 83.0 | 78.1 | 90.5 | -4.6 |

While the system level EPNL provides a starting point for investigating the differences in the TTBW and CC, comparison of the received noise levels at the observer for the individual elements in the prediction, shown in Figure 3, also provides insight. Overall, the jet and fan elements (including PAA effects and fan duct liner) are dominant at the takeoff conditions, and near parity with the airframe noise at approach. Consequently, understanding the differences at each certification point only requires the components that appreciably contribute to the system noise. While the elements comprising the engine have different levels between the TTBW and CC, the similarities in the relative magnitudes of those elements for both configurations derive from the commonality of the gFan+ engine cycles. The airframe elements have more variation in relative magnitude due to differences in design and operation (e.g., flight speed).

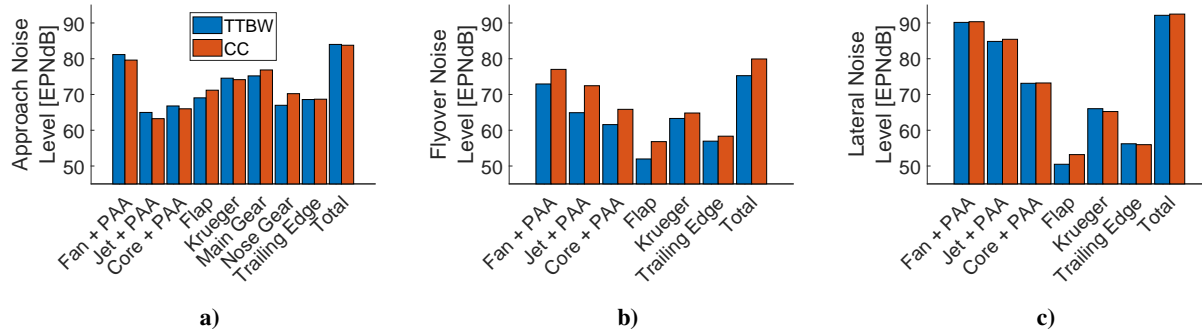


Fig. 3 The source rankings for the baseline TTBW and CC are shown at each certification point: a) approach, b) flyover, and c) lateral.

These operational differences play a key role at the system level as well, although the regulations constrain many flight parameters. On approach, aircraft must follow a fixed 3° glide path and ground intercept location. All configurations have the same propagation distance through the path, and differ only in the approach speed and power setting needed to maintain the required flight path. Similarly, the lateral point (when using the alternative procedure in 14 CFR Part 36 Section B36.3(a)(1) [28], as is done here) places the observer on a line parallel to the flight track where the aircraft reaches 985 ft altitude above ground level. Additionally, full power must be used for this flight segment, which sets the flight path angle and takeoff speed. Although the variation in flight path angle across configuration does provide some opportunity for propagation distance difference (through altitude differences), this is limited as the uniform sideline distance is a large contributor to the total propagation distance. The flyover observer, located at a fixed distance from brake release, provides the least constrained certification point in an operational sense. Notably, Table 2 shows that the largest difference in the individual certification levels is present at the flyover certification point.

The beneficial low-speed characteristics of the TTBW are enumerated by discussing each stage of the takeoff flight paths, as shown in Figure 4. Following brake release, the TTBW benefits from its higher thrust-to-weight ratio to accelerate faster than the CC. This benefit is compounded by lower wing loading, with the TTBW FAR takeoff field length 2000 ft shorter than the CC. During the full power climb segment, the improved L/D of the TTBW enables a higher rate of climb, continuing to widen the altitude gap. Following the full power segment, the engine power setting is reduced prior to passing overhead of the flyover observer. The lowest allowable power setting is the maximum of either the power required to maintain a 4% climb gradient, or level flight with one engine inoperable [28]. For both vehicles, the active constraint is the one engine inoperable condition. Again, the superior L/D of the TTBW provides an advantage, this time through a lower power setting and the corresponding reduction in source noise levels. Figure 3b) illustrates that the primary impact of the throttle setting reduction is on the jet element rather than the fan element; TTBW jet velocities and temperatures are considerably lower than the CC. The Kresja fan model primarily indicates improvements in TTBW tonal fan noise and aft broadband noise relative to the CC. It should be noted that the lower power setting does come at the cost of reducing the altitude advantage over the cutback segment. With the higher altitude and lower flight speed, the EPNL calculation for the TTBW indicates a roughly 1 EPNdB duration penalty relative to the CC. While the minimum power setting is likely to provide an overall advantage, it is of interest in future work to better understand the trade between power setting, altitude, EPNL duration, and the distance from brake release where engine cutback is initiated. Regardless, for the certification-compliant flight paths used here, the additional altitude of the TTBW when passing overhead provides an additional 2 dB advantage from spherical spreading loss. Additionally, the extra propagation distance provides the opportunity for atmospheric absorption of higher frequency (2–10 kHz) sources.

With regard to the system noise, this will primarily benefit inlet broadband fan noise, which has considerable energy in the 2–6.3 kHz bands, where the perceived noise level metric is most sensitive. The effect on aft broadband noise and tonal noise is more limited due to the Doppler shift and a fan blade passage frequency under one kilohertz. For reference, SAE ARP866A [33] estimates the additional propagation distance produces excess atmospheric attenuation of 2.4 dB and 7.3 dB for the 2 kHz and 6.3 kHz one-third octave bands, respectively, at certification atmospheric conditions.

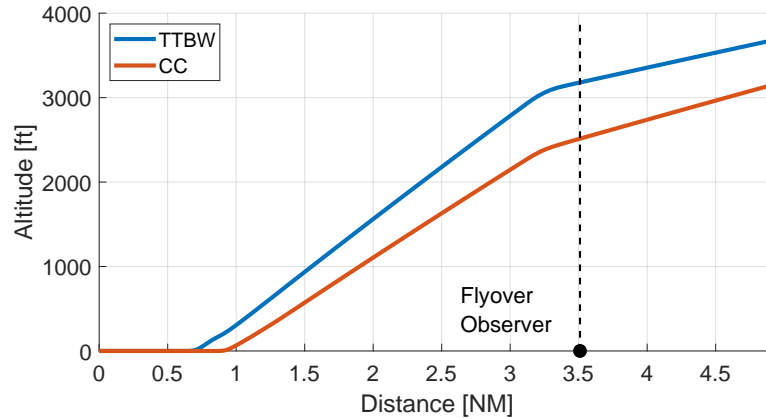


Fig. 4 The takeoff flight profiles for the TTBW and CC are shown with distance referenced to the location of brake release. Additional annotation highlights the location in the profile that is overhead of the flyover observer.

While the differences for the other two certification points are of smaller magnitude, it is still worth mentioning some of the primary differences. At the lateral point, the TTBW has higher fan and jet noise levels when PAA effects are removed from the prediction, due to the higher thrust engine sizing (see Table 1). Although the TTBW has a lower takeoff weight and better L/D performance, additional thrust is required to reach the design top of climb, 4400 ft higher than top of climb altitude for the CC. The primary impacts on the lateral certification noise due to resizing the engine are in modeling terms dependent on mass flow rate or nozzle areas, as the engine cycle temperatures and Mach numbers are constant when the same engine cycle is scaled on thrust [34]. The minor differences in cycle temperatures and Mach numbers are due to the change in flight speed on the flow into the engine, as well as modifying the strength of the bypass shear layer.

For the approach point, several factors differentiate the noise of the individual elements although the system noise is comparable. This point also has appreciable contributions from both the engine and airframe subsystems, unlike the takeoff certification points. Regarding engine noise, the TTBW has higher levels due to a slight increase in the required thrust relative to the CC. For the airframe elements, the TTBW has lower noise levels at the approach observer for all but the Krueger leading edge element. This advantage derives from the lower approach speed of the TTBW. When the EPNL levels of the TTBW airframe elements are crudely scaled to match the approach speed of the CC using a Mach number power law, sixth power for the landing gear and fifth power for the high-lift and trailing edge noise, a more understandable relation emerges. The flap and nose gear, which have similar designs across both configurations, have comparable levels. The main gear of the TTBW is louder as it is assumed that the placement under the strut does not generate significant circulation to lower the local flow velocity. The Krueger leading edge of the TTBW is louder as the design has more than double the number of brackets present on the CC. This can be seen in Figure 1, where each panel is modeled to have two brackets. Brackets for Kruegers are generally more complex than for slats, consequently the bracket noise is an important component of the Krueger element noise. Last, the trailing edge noise of the TTBW is also elevated relative to the CC; it has a much longer span, and the strut provides an additional surface to generate trailing edge noise.

B. Comparison with Phase II Results

Although an overview of the Phase II noise analysis by Boeing is provided in Section I, it is instructive to provide additional insight and caveats for comparing those results with this paper. The differences between the studies fall into two categories: design and noise modeling. On the design side, there has been significant development in subsequent phases of the SUGAR contract to modify the cruise Mach number from 0.7 to 0.8, in addition to performing detailed

design of the high-lift system layout. Although both the Phase II and current noise predictions follow the same general process of using source models for each individual element and incoherently summing after propagation to get the total system noise, there are differences in the models used by each. The Phase II prediction uses GE static engine data and Boeing prediction methods for the airframe noise; the current prediction uses parametric models available in the research version of ANOPP. For instance, rather than static engine data, the Krejsa fan prediction method used here is based on model scale data collected in the 9- by 15-Foot Low-Speed Wind Tunnel at Glenn Research Center. Additionally, the Phase II prediction did not include PAA effects.

From a cursory comparison of the cumulative margin of the Phase II and current predictions, there appears to be fair agreement, with a difference of only 2.2 EPNdB. However, when the levels at the individual certification points are compared, much larger magnitude discrepancies arise: 8.1 EPNdB, 5.1 EPNdB and 10.7 EPNdB for approach, flyover and lateral, respectively. Element level data, in the form of tone-corrected perceived noise level as a function of time, are only published in the Phase II reports for the SUGAR Volt, further complicating any direct comparisons. However, it is noted that “the results are similar for the SUGAR High [5]”. From these plots, the element source ranking is observed to be quite different between the two predictions. While the engine is still dominant on the takeoff certification points for the Phase II prediction, the system levels (set primarily by the fan and jet noise) vary significantly, pointing to differences in those particular source noise models. For the lateral point in particular, a portion of this difference is attributable to the 4000 lb thrust per engine increase of the current prediction relative to the Phase II value. However, thrust is not the only factor; the flyover and approach thrusts are more comparable. This is further reinforced by the Phase II approach results, which show much higher airframe noise relative to engine noise than is seen in the current prediction. For instance, the maximum perceived noise level at approach of the fan noise relative to that of the main gear changes by 10 TPNdB between the two predictions. Since the geometry of the main gear has not changed since Phase II, it is believed that the main gear provides the best opportunity to compare received levels of different noise source elements.

The potential issue with the prediction of the fan element (includes fan source, liner treatment, and PAA) is one that has been noted in the past, and is of particular importance to understand in the near future. While the Phase II prediction did not include PAA effects, this does not explain the differences completely. There is anecdotal evidence of either an overprediction by ANOPP of fan noise or an underprediction of the acoustic liner attenuation, or more likely, both. Clark et al. [35] evaluated the overall fan noise prediction process in ANOPP-Research, including the Krejsa method for fan source noise, GE method for liner attenuation, and a data-driven approach for PAA effects. Their comparison indicated that at high power settings, overall fan noise was overpredicted near frequencies with the most influence on EPNL calculation, although the results were also highly dependent on emission angle. The ANOPP-Research comparisons to flight test data did not model combination tones, which would extend the overprediction to lower frequencies if included. For the TTBW, removing combination tones from the lateral point ANOPP prediction yields an additional 1.7 EPNdB reduction in system noise. Additionally, it is noted that the acoustic liner model is calibrated to large commercial turbofan engine data that were available prior to publication in 1996. Since that time, several changes in design and installation (e.g., removal of barrel splices) have greatly improved the efficiency of liner treatment. While corrections have been applied to the prediction in an attempt to account for these changes, work is underway to update the fan and liner models in the near future.

C. Roadmap Results

In addition to the baseline prediction comparison, a noise technology roadmap was applied to both the TTBW and CC. The impact of each technology is tabulated in Table 3. As one-off and one-on values are generally within 0.1 EPNdB for both configurations considered here, only the one-off values are presented for brevity. The technologies that perform best at the system level are those that reduce the fan noise element, as could be expected from the baseline results. As nearly all (except the case where an incompatible technology replaces another) of the one-off technology impacts are relative to the configuration with all of the mid and potential mid term technologies applied, the source ranking is shown in Figure 5 for additional context. A comparison with Figure 3 shows that although there has been some success in reducing the dominance of the fan element for both the TTBW and CC, particularly at flyover, it still remains the best source to target for system noise reduction.

Returning to the assessment of the individual technologies, the only other results with cumulative noise reductions of 0.5 EPNdB or greater are the center plug liner, Krueger dual-use fairing, pod landing gear (TTBW only), and partial main gear fairing (CC only). Note that the airframe technologies with large system noise reductions are the two leading contributors to airframe noise in the baseline predictions. One technology that stands out as having a large difference in effectiveness in the partial main gear fairing. The fairing is relatively ineffective on the TTBW due to the differences in

Table 3 The cumulative system level impact of each technology is given in units of Δ EPNdB in the chosen buildup order for the TTBW. Potential mid term are separated from mid term technologies by the double line.

| Technology | Element | TTBW | CC |
|---------------------------|-------------------------|-------|-------|
| MDOF Liner | Fan | 1.5 | 1.2 |
| Over-the-Rotor Liner | Fan | 1.4 | 1.3 |
| Soft Vane | Fan | 0.8 | 0.6 |
| Center Plug Liner | Core | 0.7 | 0.5 |
| Core Cowl Liner | Aft Fan | 0.4 | 0.4 |
| PAA Chevrons | Jet | 0.3 | 0.3 |
| Thickened Bifurcation | Aft Fan | 0.2 | 0.3 |
| Partial Main Gear Fairing | Main Gear | 0.1 | 0.5 |
| Porous Flap Side Edge | Flap | 0.2 | 0.2 |
| Partial Nose Gear Fairing | Nose Gear | 0.1 | 0.1 |
| Landing Gear Door Liner | Main Gear | <0.05 | 0.1 |
| Krueger Dual Use Fairing | Leading Edge | 0.7 | 0.5 |
| Scarf Inlet | Forward Fan Directivity | 0.6 | 0.7 |
| Pod Landing Gear | Main Gear | 0.5 | — |
| Lip Liner | Forward Fan | 0.4 | 0.4 |
| PAA Wing Liner | Aft Fan/Core Reflection | 0.1 | 0.2 |
| Continuous Moldline Link | Flap | 0.2 | 0.3 |
| Sealed Krueger Gap | Leading Edge | <0.05 | <0.05 |

the relative importance of the main gear element to the total system noise compared to the CC. At the subsystem level, the partial main gear fairing provides comparable noise reduction impact for both configurations. This tendency of the TTBW to deemphasize the effectiveness of main gear noise reduction technologies relative to the CC serves to illustrate how effective the pod gear is at reducing the main gear element noise. At the airframe subsystem level, the impact of the pod gear is 2.0 EPNdB. The Krueger dual use fairing also has a significant cumulative impact at the airframe subsystem level, 5.7 EPNdB for the CC and 6.0 EPNdB for the TTBW. Together with the pod gear, these two technologies provide nearly all of the airframe noise reduction potential for the TTBW.

The situation of the partial main gear fairing and pod gear can be contrasted to that of the porous flap side edge and continuous moldline link technologies; for these aircraft configurations as designed, the continuous moldline link does not provide a significant advantage at either the system or airframe subsystem level despite being more effective at the element level.

Apart from showing the impacts of individual technologies, the cumulative impacts of the technology packages, mid term and potential mid term, are provided in Table 4. The mid term impact is relative to the baseline, while the potential mid term is relative to the configurations with all the mid term technologies applied, allowing the two impacts to be added together for the total amount of noise reduction available to each configuration from the total roadmap. Overall, the results are comparable, with an apparent slight advantage to the TTBW in using the technologies to more effectively reduce noise. However, it is cautioned that a more definitive conclusion on any relative advantage cannot be reached without performing an uncertainty quantification. Further, the TTBW has the advantage of an additional technology in the potential mid term package. When the pod gear is removed from the potential mid term package for the TTBW, the cumulative impact is reduced from 2.1 EPNdB to 1.7 EPNdB.

Table 4 The cumulative impacts of the technology packages are given in units of Δ EPNdB for both configurations.

| Technology Package | TTBW | CC |
|--------------------|------|-----|
| Mid Term | 5.7 | 5.4 |
| Potential Mid Term | 2.1 | 1.9 |

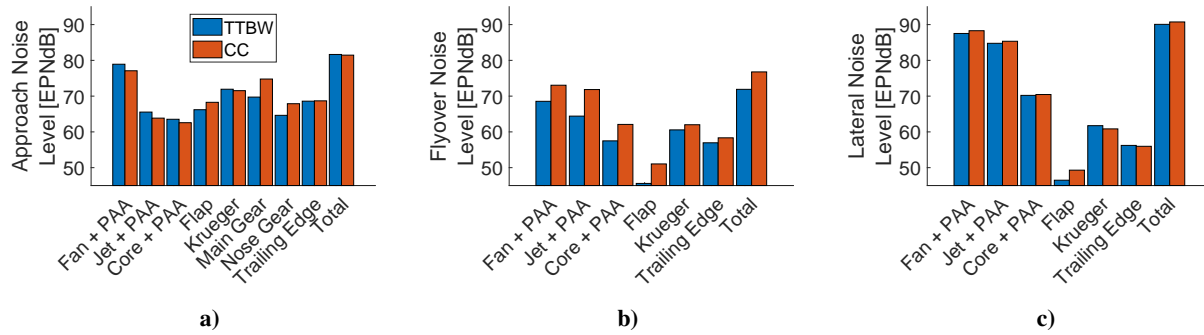


Fig. 5 The source rankings for the TTBW and CC with both mid- and potential mid term technologies applied are shown at each certification point: a) approach, b) flyover, and c) lateral.

Additionally, it is useful to contextualize the results here to both historical noise levels, as well as the NASA goals for noise reduction. Figure 6 shows the historical trend of noise reduction with the certification noise of several products [36] as a function of entry into service. The chart also shows the regulated limits on the cumulative margin as a function of time, and the NASA near-, mid-, and far term goals. Additionally, a trend line is fit through the plotted production data and extrapolated forward in time to the EIS date of the TTBW and CC. A shaded area is also extrapolated forward in time with the bounds determined by linear fits to the Boeing 737 and the Airbus A320 series products. These are chosen to estimate the range of likely results for the same single-aisle class as the TTBW and CC. For the CC, it can be seen that the baseline prediction does not improve on the margin of currently available products, but when the mid- and potential mid term technology packages are applied, the CC falls into the range of results conceivable from extrapolating forward in time. On the other hand, the baseline TTBW has a significant advantage in margin over the CC, and is predicted to have a slight improvement over currently available products. When the mid- and potential mid term technology packages are added, they meet or exceed the extrapolated trend line. However, even the quietest configurations fall well short of the NASA mid term goal, indicating that significant additional innovation in noise reduction technology is required to meet the goals with either of these configurations.

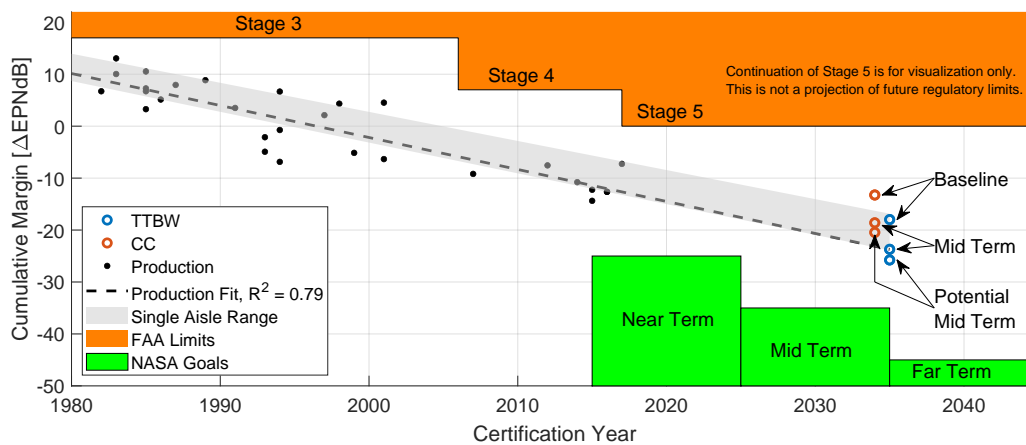


Fig. 6 The historical progress of noise reduction is shown, along with the CC and TTBW predictions with various technology packages at their entry into service date. Note that the CC results are moved forward one year to aid in reading the figure. Also shown are the NASA goals.

VI. Conclusions and Future Work

A system noise assessment and noise reduction technology roadmap development have been carried out for a transonic truss-braced wing and conventional configuration. In the baseline predictions, the TTBW was shown to have an additional cumulative margin (lower community noise) of 4.7 EPNdB over the CC. The improved low-speed performance is a significant factor in lowering noise, most directly through a higher altitude and deeper engine cutback at flyover, but also from a reduction in approach speed. The improved shielding of engine noise by the fuselage provides an additional advantage over the CC.

The application of the noise technology roadmap showed that both configurations fall well short of the NASA mid term noise reduction goal. However, with the application of the mid- and potential mid term technology packages, the TTBW was capable of outperforming the historical range of noise reduction improvements with time. Technologies that reduced the fan noise were particularly effective, given the dominance of that element in the system noise. These are the MDOF, over-the-rotor, and soft vane liners as well as the scarf inlet. The center plug liner was effective at reducing core noise, and the Krueger dual use fairing and pod gear resulted in significant noise reduction for the airframe subsystem. It is cautioned that the quantitative impact of these technologies is strongly tied to the source ranking balance. The technologies applied in this paper focused on fan noise in particular due to the baseline prediction ranking. If improvements in fan noise modeling lead to the element becoming less dominant in future predictions, the overall roadmap noise reduction potential risks becoming is likely to be less effective at the system level. However, the reduction in noise reduction potential will be more than offset by lower absolute fan noise levels and will result in a quieter vehicle. Additionally, while a reduction in fan noise would decrease the effectiveness of fan noise technologies, technologies that reduce the noise of other sources would become more effective; a completely new roadmap is not required to address a different source ranking. To meet the NASA noise goal with either of these configurations, future assessments need additional innovation to augment the list of technologies included in the current roadmap, with continued attention to the source ranking in choosing technologies to maximize noise reduction. Stated differently, the accuracy of the source ranking is key to identifying, prioritizing, and maturing those technologies that have the most potential for noise reduction.

There are many aspects of this noise assessment that can be improved in future iterations. The first is to complete an uncertainty quantification of both the baseline prediction and noise technology roadmap. In order to support risk reduction of the TTBW configuration, the relative noise levels between the TTBW and CC must be determined with high confidence so that the appropriate trades can be made. Generally, additional margin is desired for new products, as uncertainty is larger than for incremental advancement that benefits from a wealth of relevant flight test data [37].

Additionally, there must be sufficient margin to have confidence that the design meets not only the current regulations but also any more stringent regulations that may be proposed prior to entry into service. For the TTBW, the sideline margin for the baseline vehicle is 2.9 EPNdB relative to the individual margin required under Stage 5 (3.9 EPNdB to the limits defined in Stage 3), which warrants further attention to ensure that there is acceptable risk to meeting certification. Given that the CC has a similar predicted margin to the TTBW at sideline, and that recent iterations of single-aisle products have much larger margins, it is quite likely that the perceived risk stems primarily from noise prediction modeling bias rather than a true issue.

With respect to the modeling, several improvements are planned. Updates to the fan source and liner attenuation modeling are ongoing. More work is also needed to continue to improve the modeling of and understand the physics of the PAA effects for the TTBW configuration. With improved understanding, it is likely that additional technologies to limit detrimental PAA effects can be ideated and developed. Last, some of the models that have been applied to noise reduction technology could be improved through higher fidelity modeling and integration of available experimental data.

Acknowledgments

The Advanced Air Transport Technology Project is acknowledged for funding this work. The authors would like to thank the technical reviewers, and all who contributed to this work. The authors would also like to thank Rob Thacker for his contribution of engine sizing, Nat Blaesser for his work on aircraft sizing and flight paths for the TTBW, as well as Tom Ozoroski for the aircraft sizing and flight path of the conventional configuration. Additionally, the authors would like to thank Ty Marien and Jesse Quinlan for their efforts in coordinating development of both configurations.

References

- [1] National Aeronautics and Space Administration, "NASA Aeronautics: Strategic Implementation Plan," 2019, pp. 37–43. URL

<https://www.nasa.gov/aeroresearch/strategy>.

- [2] Carrier, G., Atinault, O., Dequand, S., Hantrais-Gervois, J.-L., Liauzun, C., Paluch, B., Rodde, A.-M., and Toussaint, C., "Investigation of a Strut-Braced Wing Configuration for Future Commercial Transport," *28th International Congress of the Aeronautical Sciences*, 2012. URL https://www.icas.org/ICAS_ARCHIVE/ICAS2012/PAPERS/597.PDF.
- [3] Ricci, S., "Recent Achievements in the Design of Ultra High Aspect Ratio Wings of Environmental Friendly Aircraft," *Presented at the 11th EASN Virtual International Conference*, 2021. doi:10.5281/zenodo.5706398.
- [4] Bradley, M. K., and Droney, C. K., "Subsonic Ultra Green Aircraft Research: Phase I Final Report," NASA/CR-2011-216847, April 2011. URL <https://ntrs.nasa.gov/citations/20110011321>.
- [5] Bradley, M. K., and Droney, C. K., "Subsonic Ultra Green Aircraft Research: Phase II - Volume II - Hybrid Electric Design Exploration," NASA/CR-2015-218704/Volume II, April 2015. URL <https://ntrs.nasa.gov/citations/20150017039>.
- [6] Droney, C. K., Sclafani, A. J., Harrison, N. A., Grasc, A. D., and Beyar, M. D., "Subsonic Ultra Green Aircraft Research: Phase III - Mach 0.75 Transonic Truss-Braced Wing Design," NASA/CR-2020-5005698, September 2020. URL <https://ntrs.nasa.gov/citations/20205005698>.
- [7] Harrison, N. A., Gatlin, G. M., Viken, S. A., Beyar, M., Dickey, E. D., Hoffman, K., and Reichenbach, E. Y., "Development of an Efficient M=0.80 Transonic Truss-Braced Wing Aircraft," *AIAA Paper 2020-0011*, January 2020. doi:10.2514/6.2020-0011.
- [8] McCullers, L., "Aircraft Configuration Optimization Including Optimized Flight Profiles," *Proceedings of the Symposium of Recent Experiences in Multidisciplinary Analysis and Optimization*, NASA CP-2327, 1984, pp. 395-412. URL <https://ntrs.nasa.gov/citations/19870002310>.
- [9] Lytle, J. K., "The Numerical Propulsion System Simulation: An Overview," NASA TM-2000-209915, June 2000. URL <https://ntrs.nasa.gov/citations/20000063377>.
- [10] Welstead, J., and Felder, J. L., "Conceptual Design of a Single-Aisle Turboelectric Commercial Transport with Fuselage Boundary Layer Ingestion," *AIAA Paper 2016-1027*, January 2016. doi:10.2514/6.2016-1027.
- [11] Thacker, R., and Blaesser, N. J., "Modeling of a Modern Aircraft Through Calibration Techniques," *AIAA Paper 2019-2984*, June 2019. doi:10.2514/6.2019-2984.
- [12] Dickey, E. D., and Beyar, M. D., "SUGAR Phase IV Final Report, Volume 3 Mach 0.8 Transonic Truss-Braced Wing High-Lift System Aerodynamic Design Report," NASA Contractor Report, Unpublished.
- [13] Droney, C. K., and Zidovetzki, E. S., "SUGAR Phase IV Mach 0.80 Transonic Truss-Braced Wing Concept Data Package," NASA Contractor Report, Unpublished.
- [14] Droney, C. K., and Zidovetzki, E. S., "SUGAR Phase IV Mach 0.80 Conventional Concept Data Package," NASA Contractor Report, Unpublished.
- [15] Lopes, L. V., and Burley, C. L., "ANOPP2 User's Manual, Version 1.2," NASA/TM-2016-219342, October 2016. URL <https://ntrs.nasa.gov/citations/20160014858>.
- [16] Thomas, R. H., Guo, Y., Berton, J., and Fernandez, H., "Aircraft Noise Reduction Technology Roadmap Toward Achieving the NASA 2035 Goal," *AIAA Paper 2017-3193*, June 2017. doi:10.2514/6.2017-3193.
- [17] Guo, Y., Thomas, R. H., Clark, I. A., and June, J. C., "Far-Term Noise Reduction Roadmap for the Midfuselage Nacelle Subsonic Transport," *Journal of Aircraft*, Vol. 56, No. 5, 2019, pp. 1893-1906. doi:10.2514/1.C035307.
- [18] Clark, I. A., Thomas, R. H., and Guo, Y., "Far Term Noise Reduction Roadmap for the NASA D8 and Single-Aisle Tube-and-Wing Aircraft Concepts," *AIAA Paper 2019-2427*, May 2019. doi:10.2514/6.2019-2427.
- [19] June, J. C., Thomas, R. H., Guo, Y., and Clark, I. A., "Far Term Noise Reduction Technology Roadmap for a Large Twin-Aisle Tube-and-Wing Subsonic Transport," *AIAA Paper 2019-2428*, May 2019. doi:10.2514/6.2019-2428.
- [20] Krejsa, E. A., and Stone, J. R., "Enhanced Fan Noise Modeling for Turbofan Engines," NASA/CR-2014-218421, December 2014. URL <https://ntrs.nasa.gov/citations/20150000884>.
- [21] Heidmann, M. F., "Interim Prediction Method for Fan and Compressor Source Noise," NASA TM X-71763, June 1975. URL <https://ntrs.nasa.gov/citations/19750017876>.

- [22] Kontos, K. B., Kraft, R. E., and Gliebe, P. R., “Improved NASA-ANOPP Noise Prediction Computer Code for Advanced Subsonic Propulsion Systems, Vol. 2: Fan Suppression Model Development,” NASA CR-202309, December 1996. URL <https://ntrs.nasa.gov/citations/19970005047>.
- [23] Bilwakesh, K. R., Emmerling, J. J., Kazin, S. B., Iatham, D., Matta, R. K., and Morozumi, H., “Core Engine Noise Control Program, Vol. 3: Prediction Methods,” FAA/RD-74/125, 1976.
- [24] Stone, J. R., Krejsa, E. A., Clark, B. J., and Berton, J. J., “Jet Noise Modeling for Suppressed and Unsuppressed Aircraft in Simulated Flight,” NASA/TM-2009-215524, March 2009. URL <https://ntrs.nasa.gov/citations/20090015381>.
- [25] Guo, Y., Burley, C. L., and Thomas, R. H., “Landing Gear Noise Prediction and Analysis for Tube-And-Wing and Hybrid-Wing-Body Aircraft,” *AIAA Paper 2016–1273*, January 2016. doi:10.2514/6.2016-1273.
- [26] Guo, Y., Burley, C. L., and Thomas, R. H., “Modeling and Prediction of Krueger Device Noise,” *AIAA Paper 2016–2957*, May 2016. doi:10.2514/6.2016-2957.
- [27] Fink, M. R., “Airframe Noise Prediction Method,” FAA-RD-77-29, March 1977.
- [28] *Noise Standards: Aircraft Type and Airworthiness Certification*, Code of Federal Regulations, Title 14, Chapter I, Part 36, January 2021.
- [29] Thomas, R. H., Czech, M. J., and Doty, M. J., “High Bypass Ratio Jet Noise Reduction and Installation Effects Including Shielding Effectiveness,” *AIAA Paper 2013–0541*, January 2013. doi:10.2514/6.2013-541.
- [30] Adib, M., Catalano, F., Hileman, J., Huff, D., Ito, T., Joselzon, A., Khaletskiy, Y., Michel, U., Mongeau, L., and Tester, B. J., “Novel Aircraft Noise Technology Review and Medium and Long Term Noise Reduction Goals,” Report to CAEP by the Second CAEP Noise Technology Independent Expert Panel, ICAO Document 10017, 2014. URL https://www.icao.int/publications/Documents/10017_cons_en.pdf.
- [31] “CLEEN III Projects with Noise Goals,” *Airport Noise Report*, Vol. 33, No. 30, 2021.
- [32] Yu, J. C., Wahls, R. A., Esker, B. M., Lahey, L. T., Akiyama, D. G., Drake, M. L., and Christensen, D. P., “Total Technology Readiness Level: Accelerating Technology Readiness for Aircraft Design,” *AIAA Paper 2021–2454*, August 2021. doi:10.2514/6.2021-2454.
- [33] *Standard Values of Atmospheric Absorption as a Function of Temperature and Humidity*, Society of Automotive Engineers, March 1975. Aerospace Recommended Practice 866, Revision A.
- [34] Brandt, D. E., and Wesorick, R. R., “GE Gas Turbine Design Philosophy,” GER-3434D, 1994.
- [35] Clark, I. A., Thomas, R. H., and Guo, Y., “Fan Acoustic Flight Effects on the PAA & ASN Flight Test,” *To be presented at the 28th AIAA/CEAS Aeroacoustics Conference*, June 2022.
- [36] Hileman, J., “Addressing Aircraft Noise in the United States: Part II Mitigation Solution Development,” *Presented at the 22nd Workshop of the Aeroacoustics Specialists Committee of the CEAS*, 2018.
- [37] Hodge, C. G., “Quiet Aircraft Design and Operational Characteristics,” *Aeroacoustics of Flight Vehicles: Theory and Practice, Volume 2: Noise Control*, edited by H. H. Hubbard, 1995, Chap. 18, p. 393.